Applications of Type I diffracted photons in astronomical imaging

Eugen Pavel

Storex Technologies, Bucharest, Romania

AIRA Seminar - March 27, 2024, Bucharest, Romania

Summary

- Introduction
- Modified Thomas Young's double-slit experiment
- QCE image sensor
- Calibrations in optical microscopy
- Measurements with Type I diffracted photons in astronomical imaging
- Insensitivity of QCE image sensor to seeing conditions
- Conclusions

Introduction (1)

- Christiaan Huygens (1690)
- Isaac Newton (1704)
- Thomas Young (1803); August Fresnel (1815)
- Albert Einstein (1905); Arthur H. Compton (1923)

Introduction (2)

Optical lithography

The resolution of the smallest printable feature is calculated by Rayleigh scaling equation:

$$D = k_1 \lambda / NA$$

where k_1 is a process parameter, λ is the light wavelength and NA is the numerical aperture of the optical system. With the parameters k_1 = 0.35, λ = 650 nm, NA =0.6, we obtain **D= 379 nm**.

The quantum confinement effect (QCE) applied in Quantum Optical Lithography broke the diffraction limit.

Introduction (3)- Quantum Optical Lithography

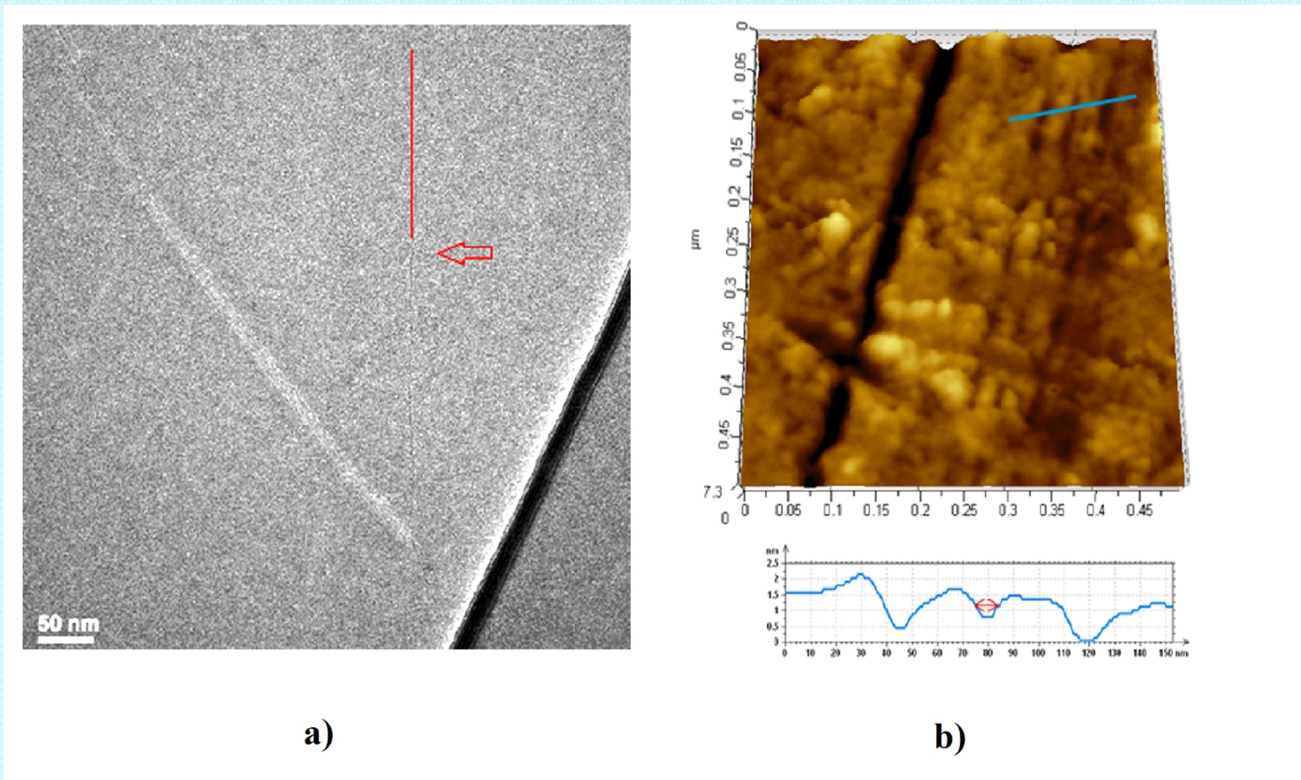

(a) TEM image of single 1 nm line. Ref. *Optics & Laser Technology* **60** (2014) 80–84; (b) AFM topography image of 2 nm parallel lines on sample surface. The cross-sections of 2 nm lines reveal line depths up to 1.5 nm – as deep as the tip can reach - and a width of 4-8 nm, broadened by the AFM tip. The thick line situated on the left size in both images represents a 20 nm marker line. Ref. *Optics Communications* **291** (2013) 259–263.

Introduction (4)- Quantum Optical Lithography

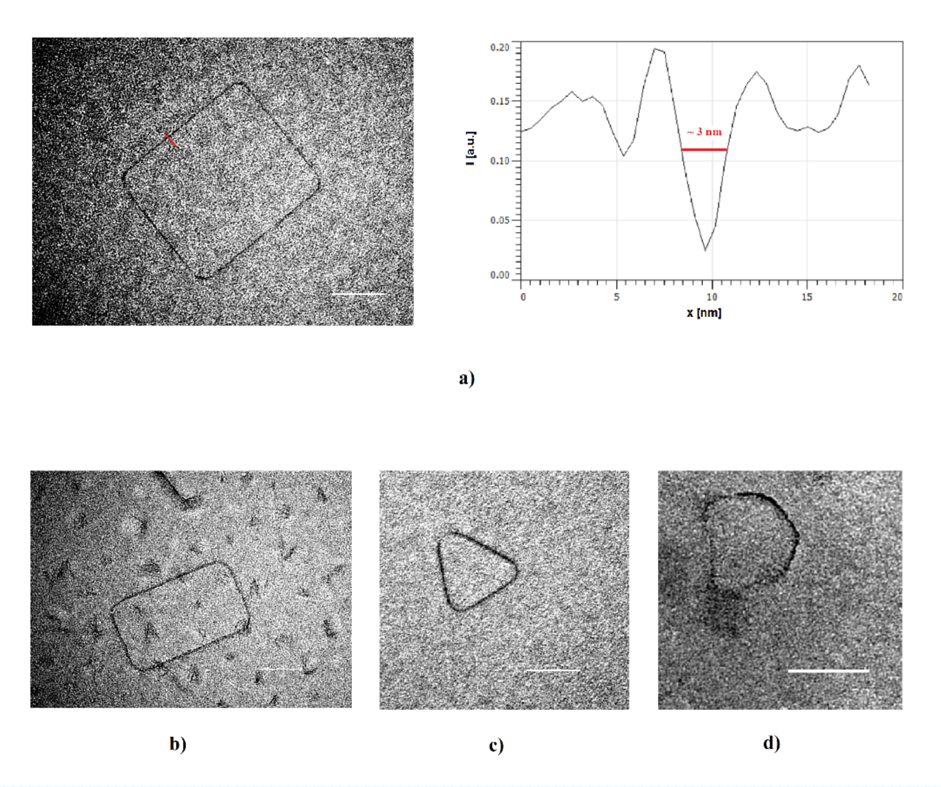

TEM images of different geometrical shapes written on Si_3N_4 TEM grids covered by resist: (a, b) rectangles written at 560nW (scale bar, 100 nm); (c) triangle written at 510 nW. (scale bar, 100 nm); (d) ”D” letter written at 510 nW (scale bar, 50 nm). Ref. *J. Micro/Nanolith. MEMS MOEMS,* **18**(2) (2019) 02050.

Modified Thomas Young's double-slit experiment (1)

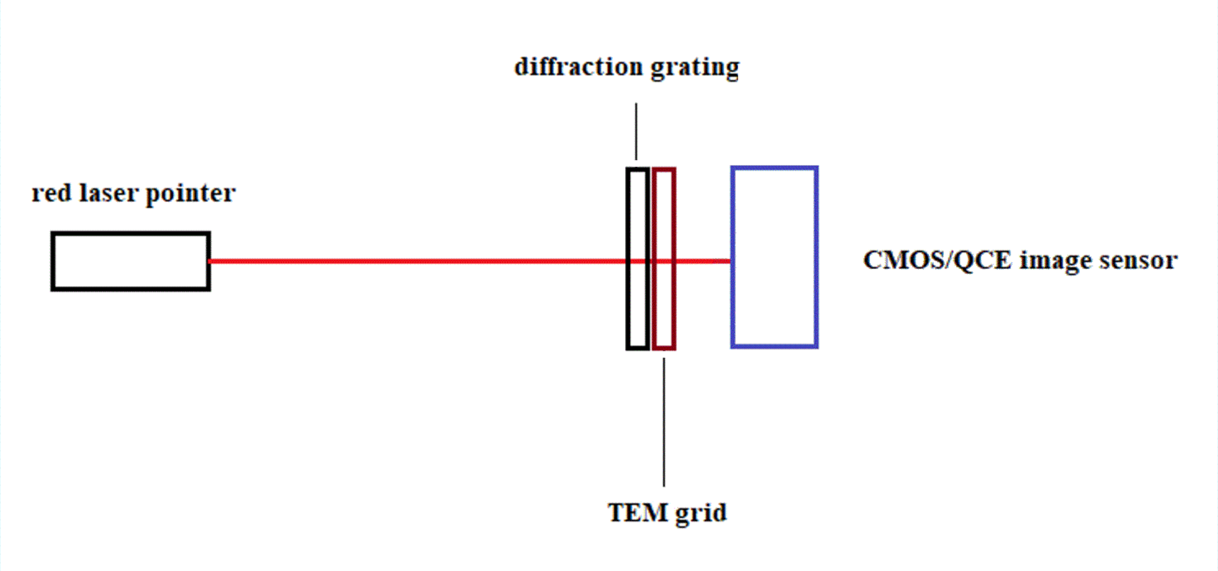

Experimental system used in multiple slit measurements.

E. Pavel, Suppression of wave-particle duality in multiple slit experiments, *JOSA B*, **41**, 547-551 (2024).

Modified Thomas Young's double-slit experiment (2)

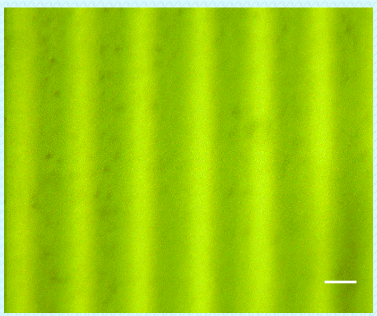

a)

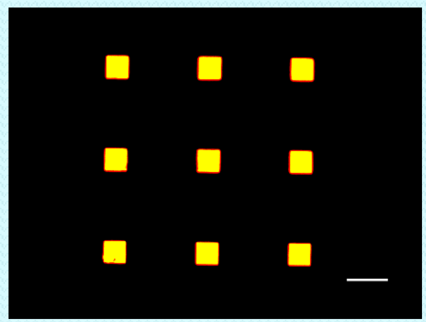

b)

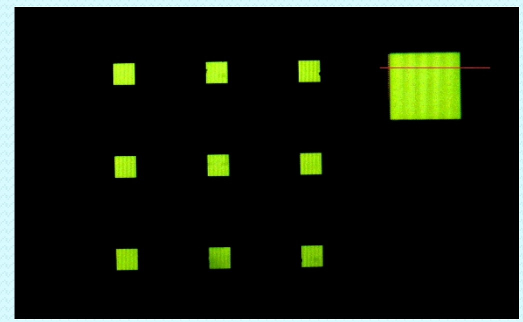

c)

Optical microscope images of: a) 50L grating, scale bar: 10 μm; b) TEM grid, scale bar: 200 μm; c) ensemble of 50L grating and TEM grid; insert: detailed image of a window.

Modified Thomas Young's double-slit experiment (3)

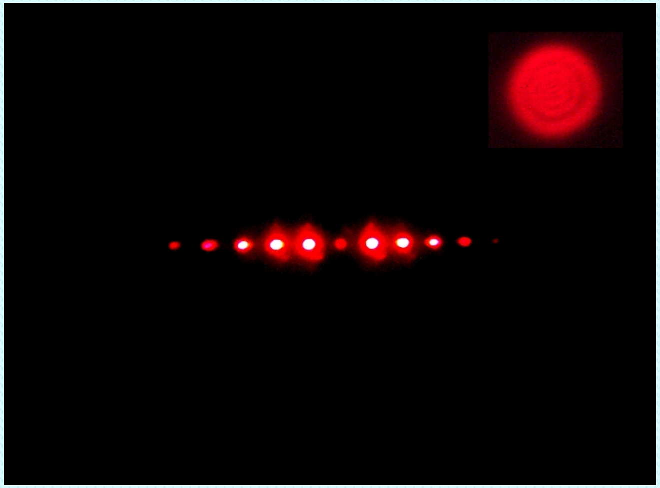

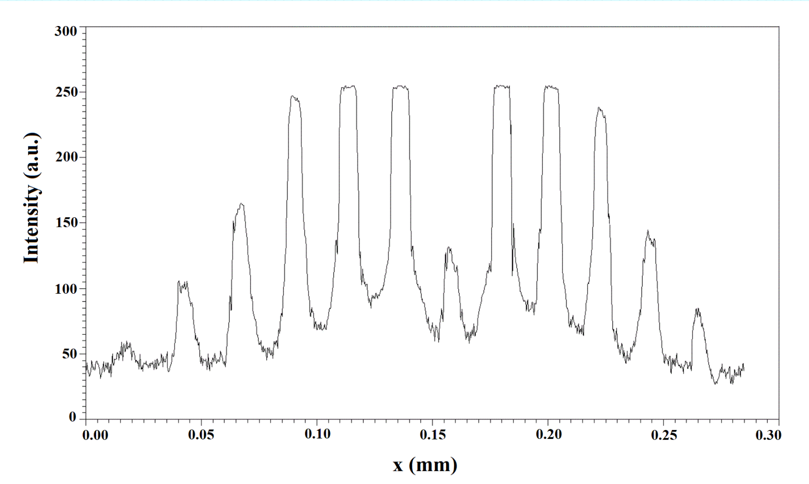

a) b)

a) Diffraction pattern of the laser pointer recorded in transmittance mode from 50L grating. The distance from the grating to the screen was D_1 = 250 mm. Insert: CMOS sensor image of TEM (4,0) cylindrical transversal mode of the laser beam; b) diffraction efficiency of grating (0, 1, 2, 3, 4, 5 orders).

Modified Thomas Young's double-slit experiment (4)

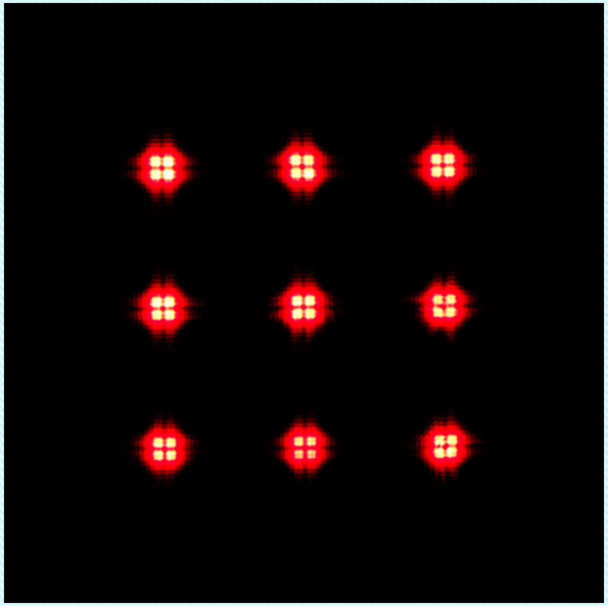

a)

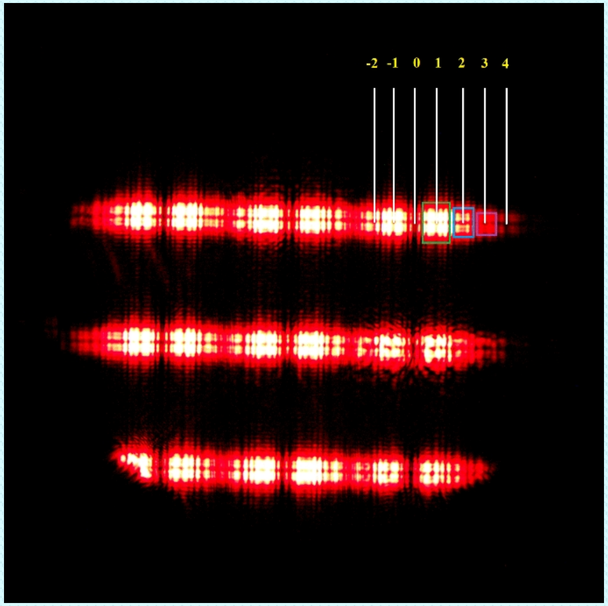

b)

a) CMOS image of the rectangular transverse mode TEM (1,1) recorded in transmittance mode from TEM grid; b) CMOS image of the diffraction patterns recorded in transmittance mode from 50L grating and TEM grid ensemble.

Modified Thomas Young's double-slit experiment (5)

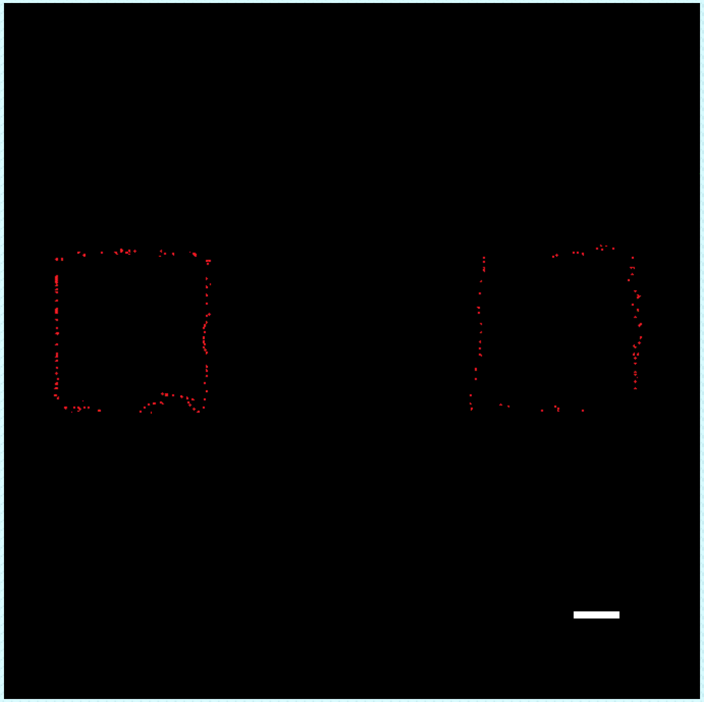

a)

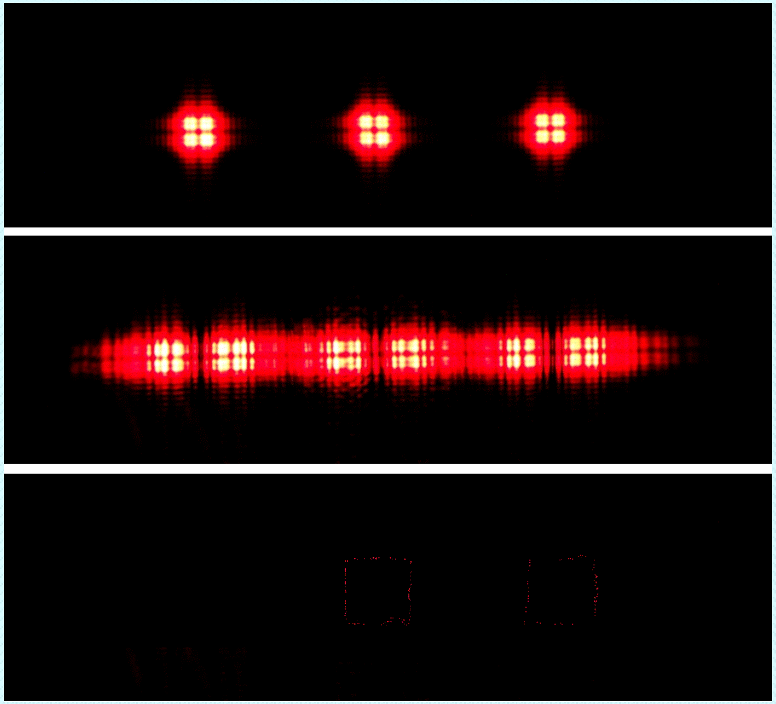

b)

a) QCE image of the pattern recorded in transmittance mode from 50L grating and TEM grid sandwich; b) rows of CMOS images of 3 windows of TEM grid without (upper row) and with diffraction grating (middle row) and QCE image with diffraction grating (lower row).

Modified Thomas Young's double-slit experiment (6)

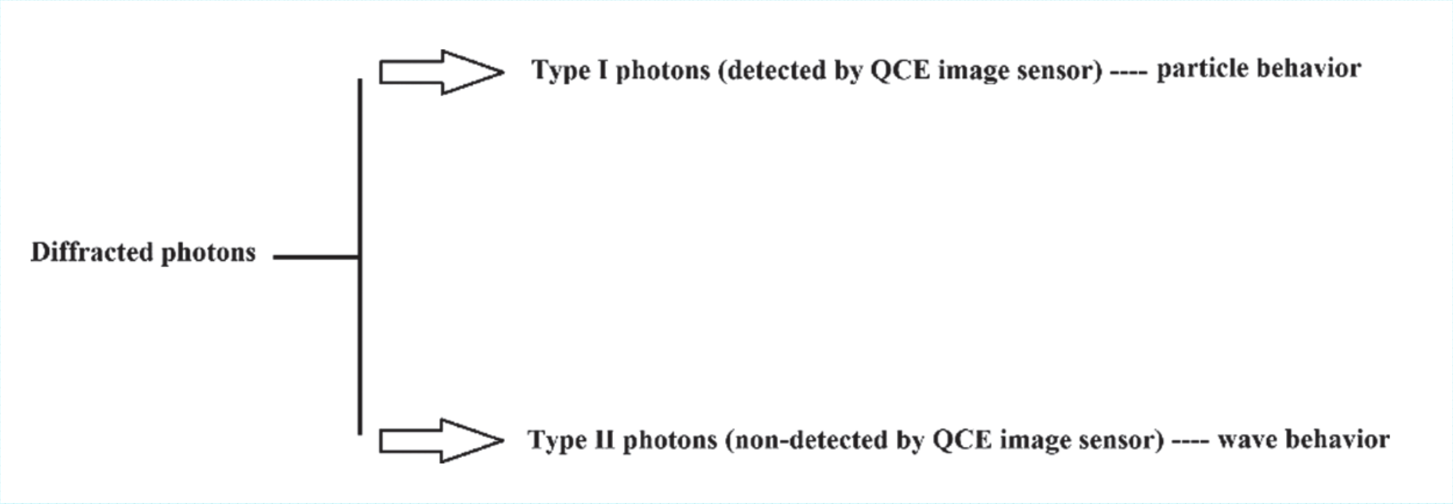

Classification of the diffracted photons.

Modified Thomas Young's double-slit experiment (7)

Table 1. Characteristics of the Diffracted Photon Types

	Detector(s)	Linear Momentum of Diffracted Photons	Fluence (Energy Delivered per Unit Area)
Type I diffracted photons	QCE image sensor	Initial	$k \times F_0^{1/3}$ [16]
Type II diffracted photons	CMOS, CCD, photographic plate, eye, etc.	Modified	$F_0 - k \times F_0^{1/3}$

QCE image sensor (1)

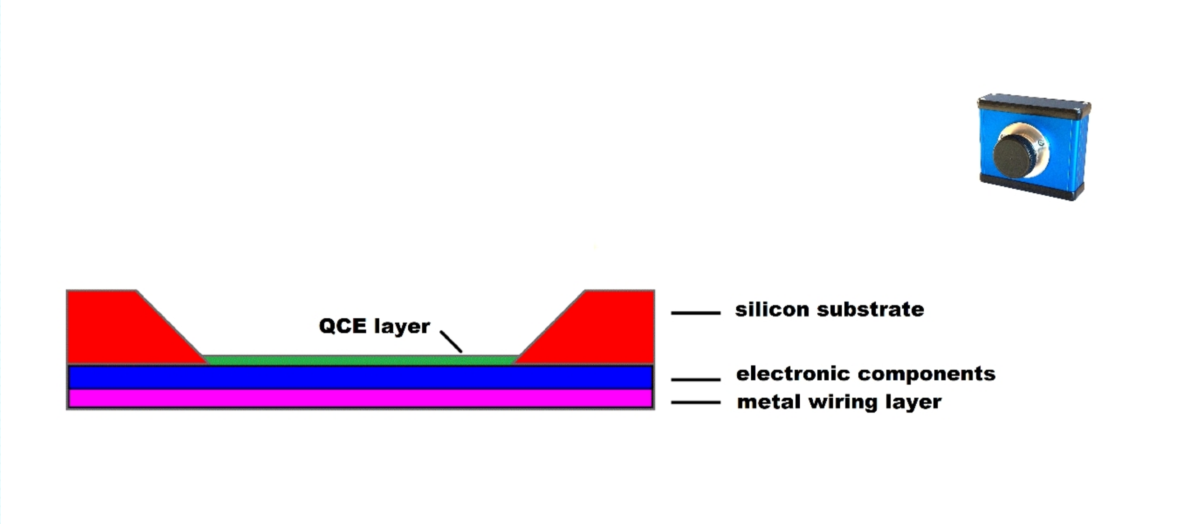

Schematic cross section of BSI QCE image sensor.

E. Pavel and V. Marinescu, Beyond the diffraction limit with quantum confinement effect (QCE) image sensor, *JOSA B*, **41**, 566-570 (2024).

QCE image sensor (2)

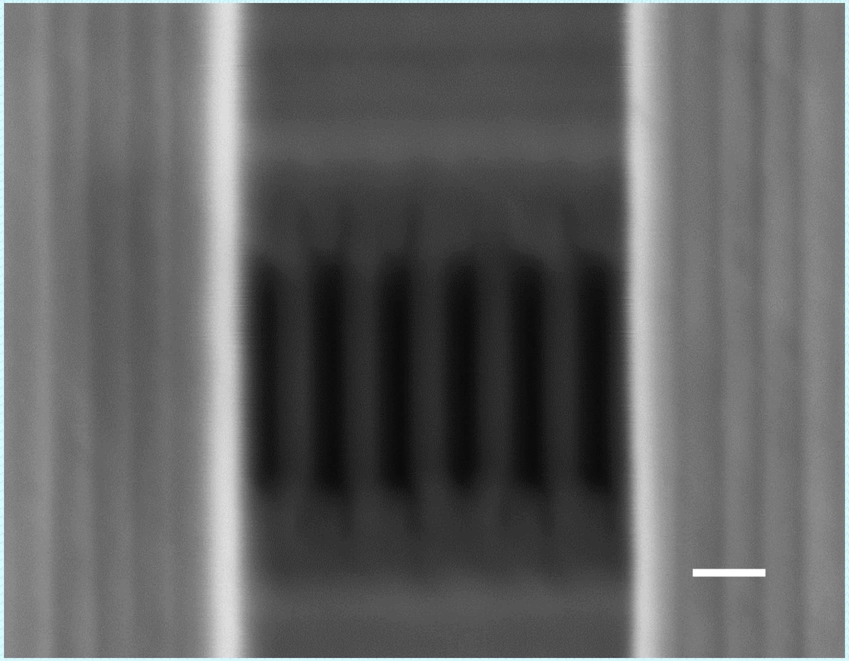

SEM image of 1Gb Winbond 25N01GVSFIT NAND memory.
Word lines have a width of 45 nm (scale bar: 100 nm).

QCE image sensor (3)

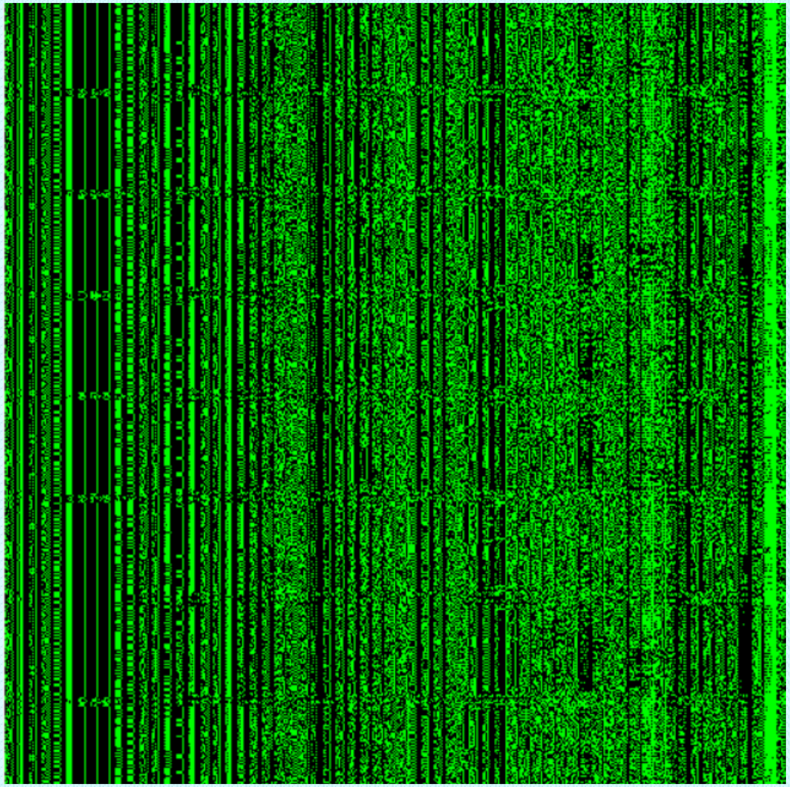

Image of a memory zone with 512 x 512 cells.

Calibrations in optical microscopy (1)

Objective	40x
NA	0.65
Diffraction limit*(nm)	619
Image resolution with A5314UPB 1.4MPixel CCD camera (nm/pixel)	168
Image resolution with QCE ST01D9 1GPixel image sensor (nm/pixel)	8.3
Magnification of QCE ST01D9 1GPixel image sensor vs diffraction limit (x)	74

Table1. Characteristics of the system composed of optical microscope and camera.

*R=0.61x λ/NA, λ=660nm;

Pixel dimension: i) A5314UPB 1.4MPixel CCD camera: 4.65 μm.

ii) QCE STM01D9 1GPixel image sensor: 60 nm, 76 times smaller than the pixel of A5314UPB 1.4MPixel CCD camera.

Calibrations in optical microscopy (2)

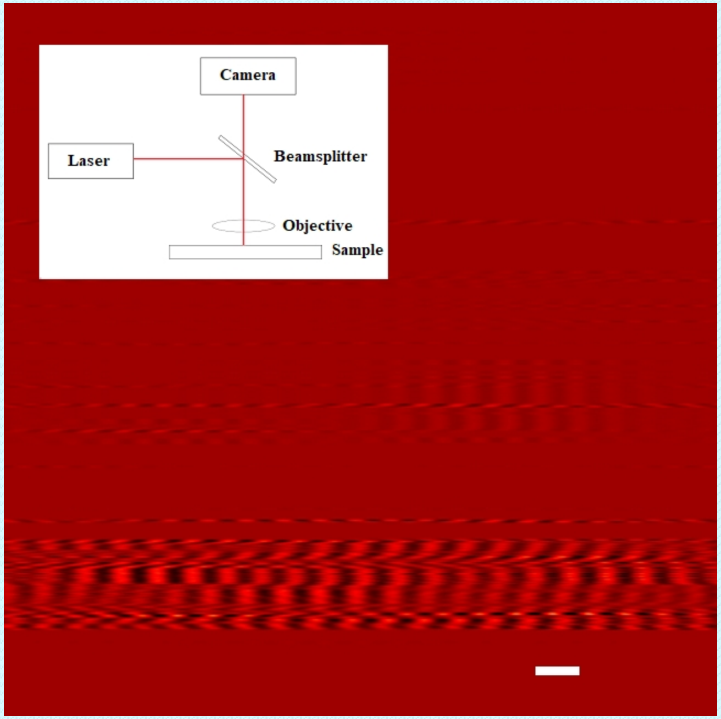

Sensor image of CD-R, objective 40x, scale bar 2 μm.

Calibrations in optical microscopy (3)

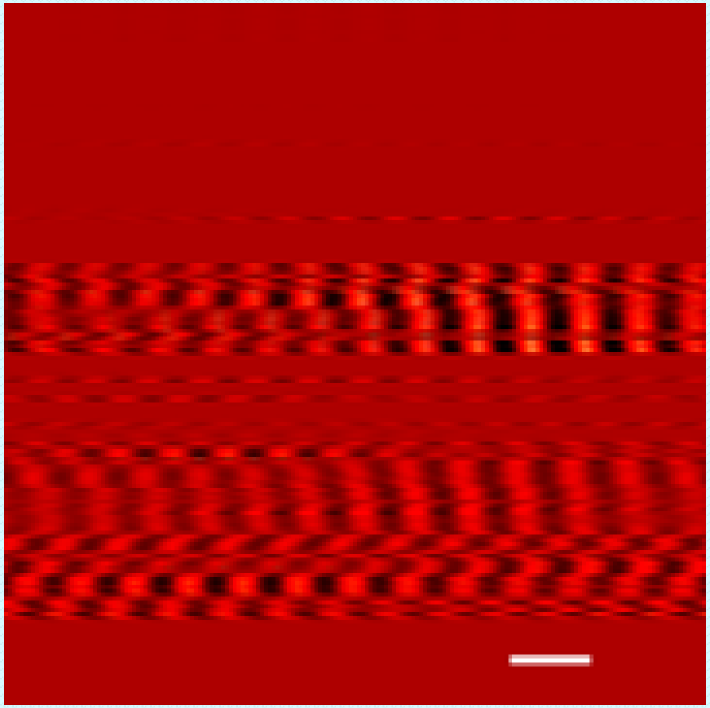

Sensor image of Blu-Ray sample, objective 40x, scale bar: 500 nm.

Measurements with Type I diffracted photons in astronomical imaging (1)

Table 1. Characteristics of the potential astronomical applications of ST01D9 1GPixel QCE image sensor

	Gran Telescopico Canarias	**Hubble Space Telescope**	**J. Webb Space Telescope**	**N150/750 with 2X Barlow lens**	**Refractor 50/600**
Φ(mm)	10400	2400	6500	150	50
Focal ratio (F/D)	16.33	24	20.2	10	12
Optimal pixel dimension* (µm)	9.96	14.6	12.3	6.1	7.32
Diffraction-limited resolution (arcsecond)**	0.012	0.052	0.019	0.838	2.516
Amplification factor*** (x)	120	175	148	73	88
Theoretical angular resolution with ST01D9 1GPixel QCE image sensor (arcsecond)	0.000100	0.000297	0.000128	0.011402	0.028590

* Optimal pixel dimension at λ= 500 nm: d(µm) =0.61x(F/D).
** Rayleigh formula at λ = 500 nm.
*** Optimal pixel dimension divided by mean pixel dimension (83 nm) of ST01D9 1GPixel QCE image sensor.

Measurements with Type I diffracted photons in astronomical imaging (2)

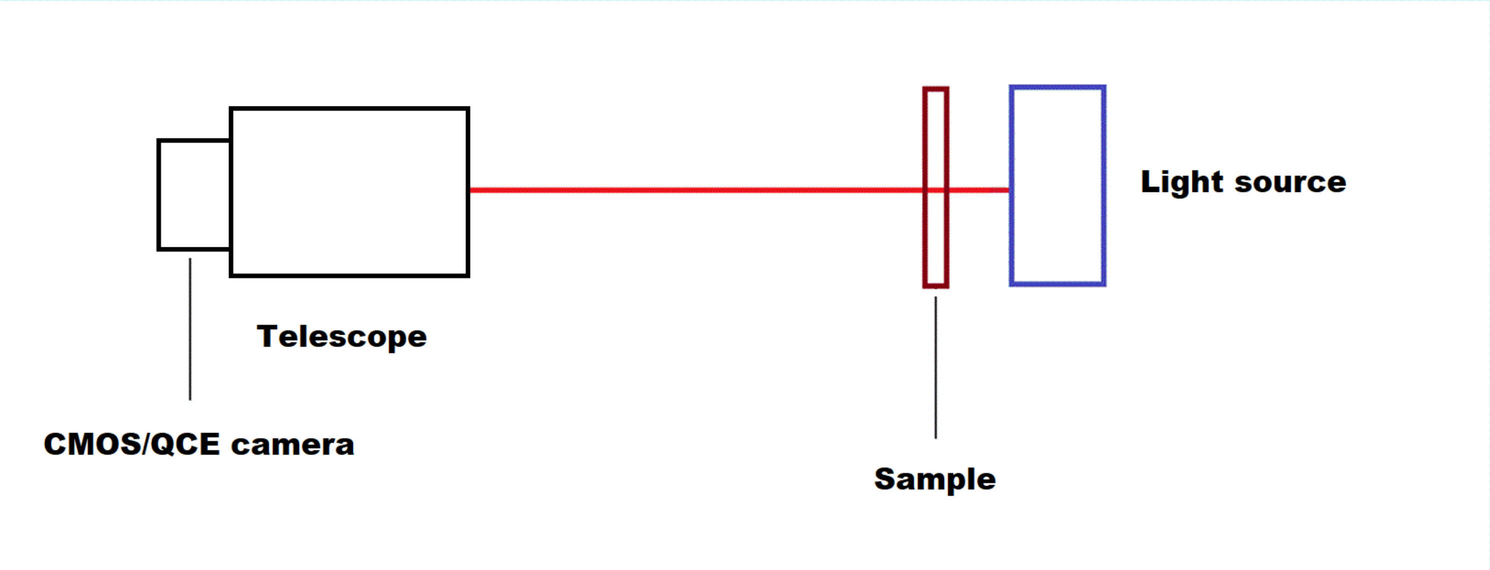

Experimental setup used in indoor measurements.

Measurements with Type I diffracted photons in astronomical imaging (3)

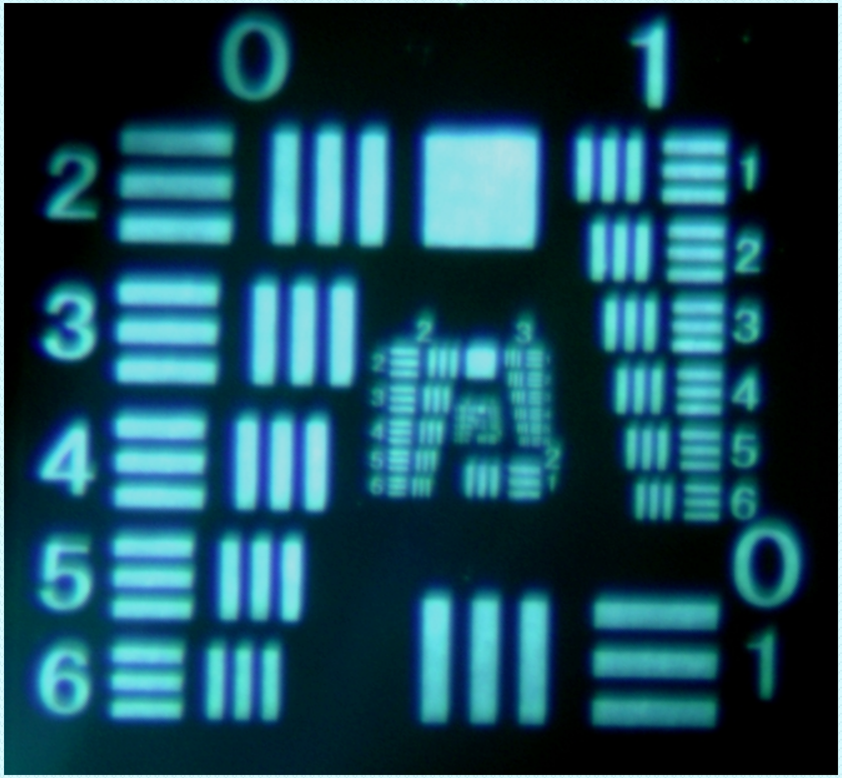

Width of a line, in millimetres,

$L\ (G;\ E)\ (mm) = 2^{-G-(E+5)/6}$

where G is the group number and E is the element number within the group.

The measured angular resolution of L(3,5) is θ = 0.804 arcsecond, close to Rayleigh diffraction limit θ = 0.838 arcsecond and Dawes' limit θ = 0.773 arcsecond.

CMOS camera image of 1951 USAF resolution test chart situated at 10 m from a N150/750 telescope with 2X Barlow lens.

Measurements with Type I diffracted photons in astronomical imaging (4)

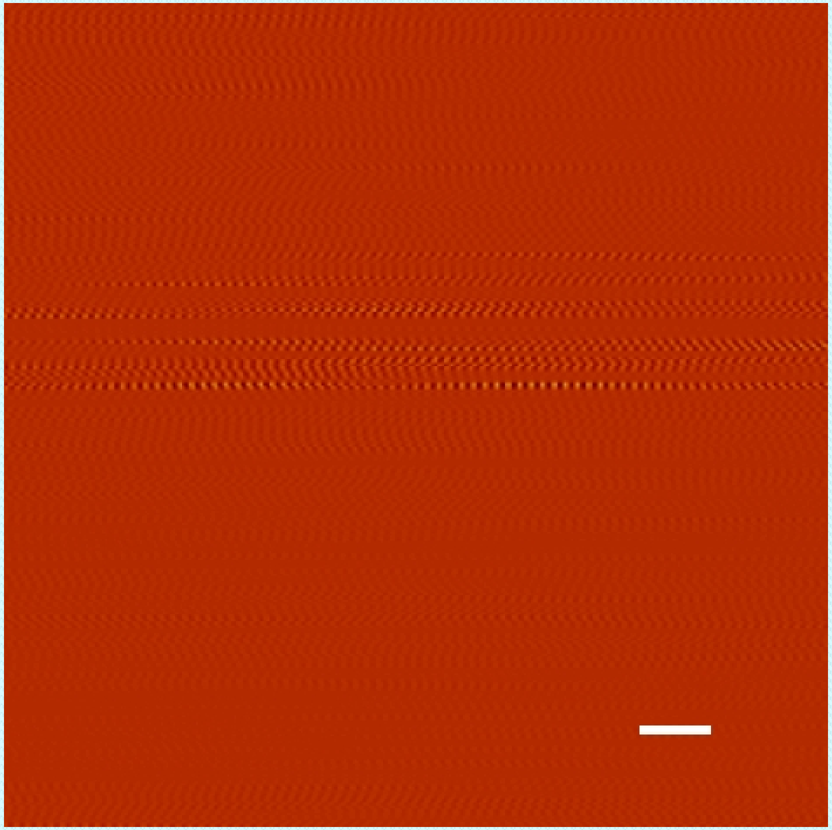

The picture captured by QCE camera of a CD-ROM sample situated at 10 m from a N150/750 telescope with 2X Barlow lens (scale bar: 200 mas).

Measurements with Type I diffracted photons in astronomical imaging (5)

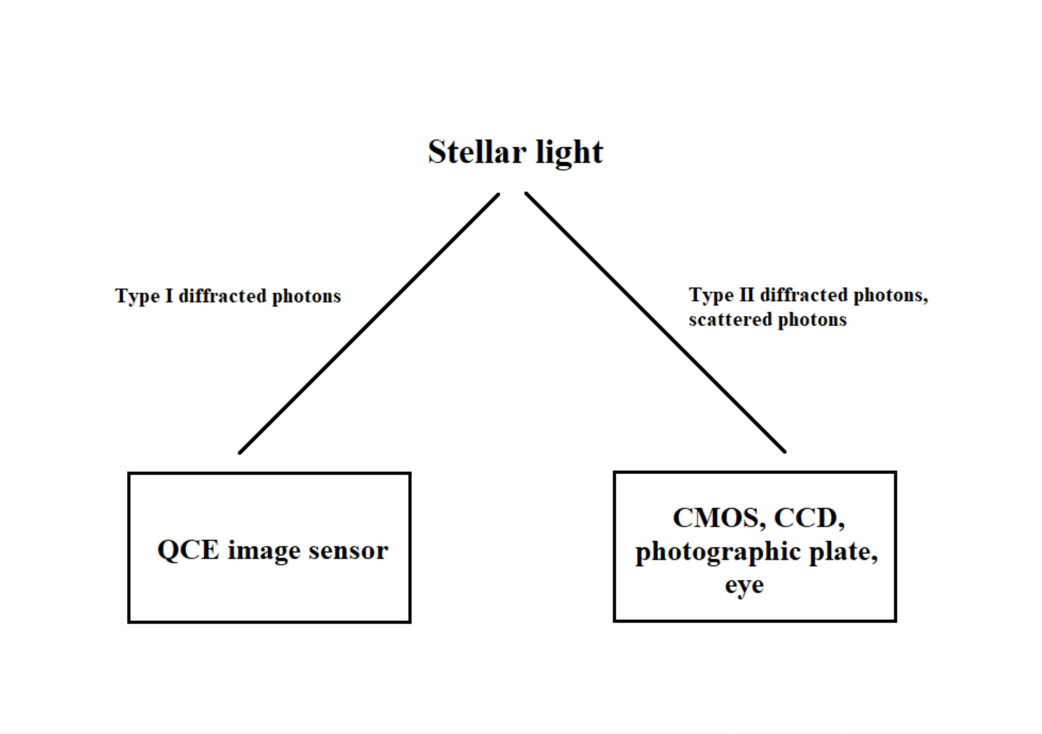

Classification of the light detectors versus photons types.

Measurements with Type I diffracted photons in astronomical imaging (6)

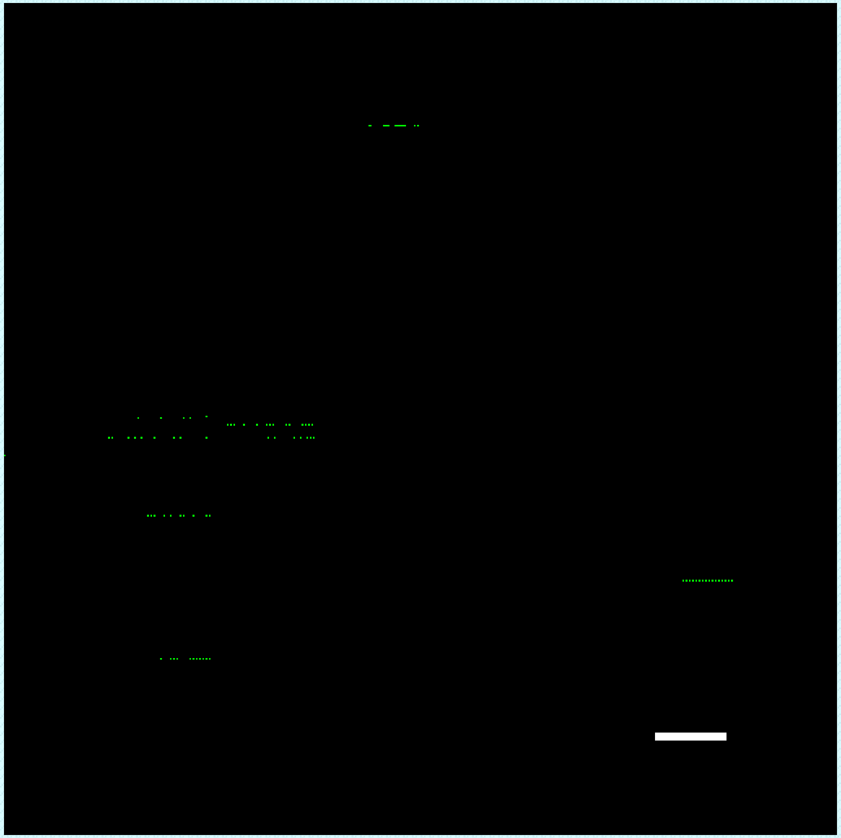

Multiple passages of Sirius (α Canis Majoris) captured by a QCE camera connected to N150/750 telescope with 2X Barlow lens (scale bar: 500 mas).

Insensitivity of QCE image sensor to seeing conditions (1)

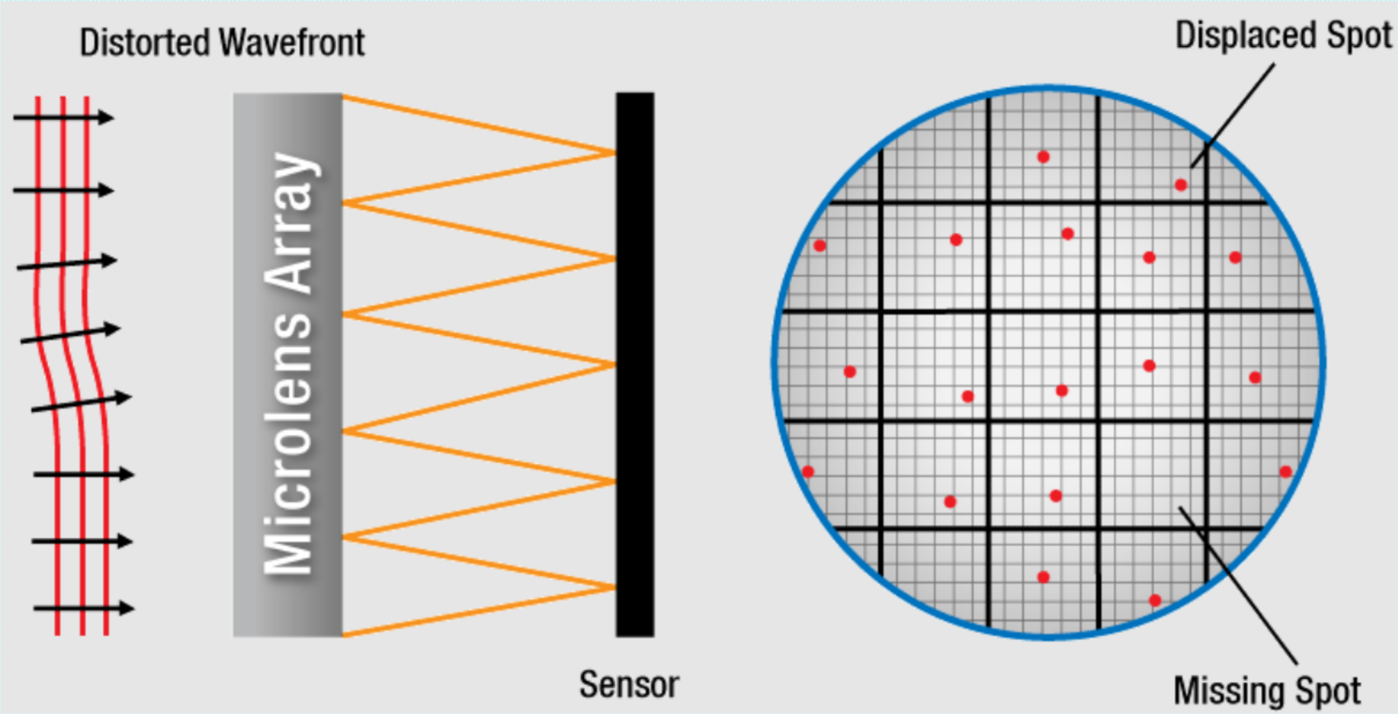

Shack Hartmann wavefront sensor.

Ref. https://www.thorlabs.com/newgrouppage9.cfm?objectgroup_id=5287

Insensitivity of QCE image sensor to seeing conditions (2)

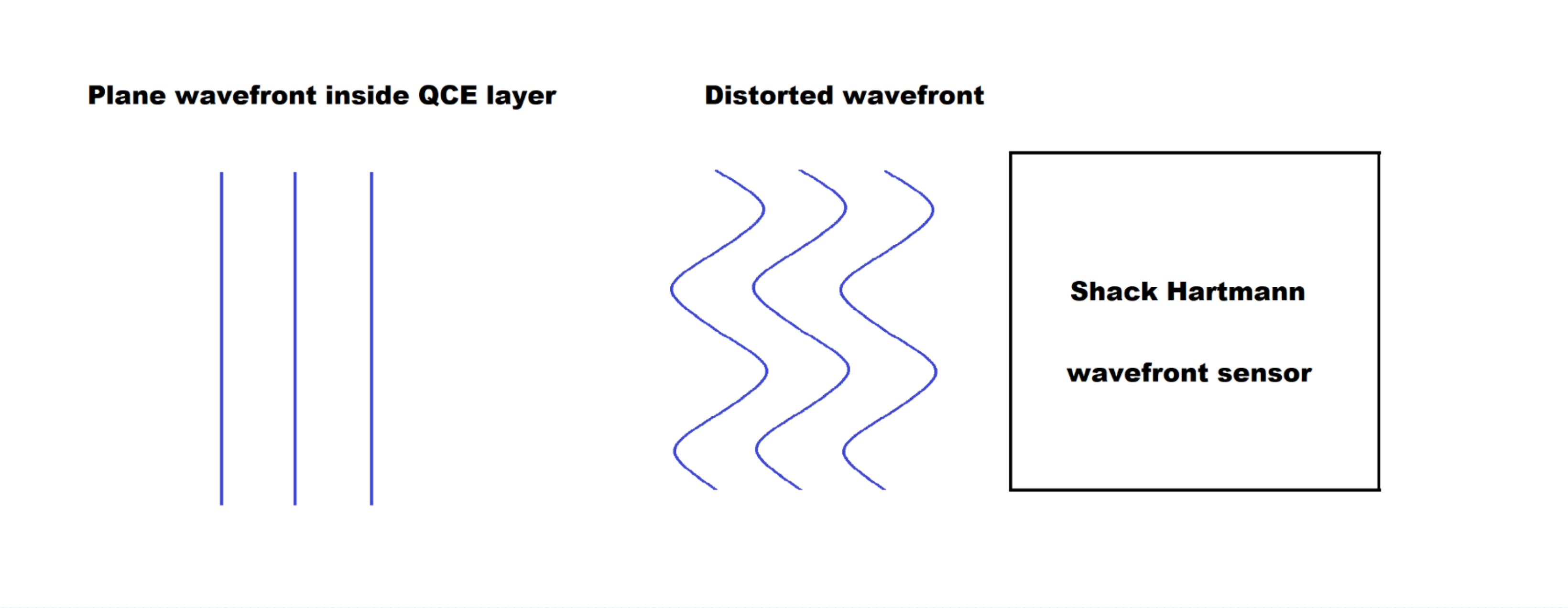

Wavefronts inside QCE layer and before Shack Hartmann wavefront sensor.

Insensitivity of QCE image sensor to seeing conditions (3) – Earth observations

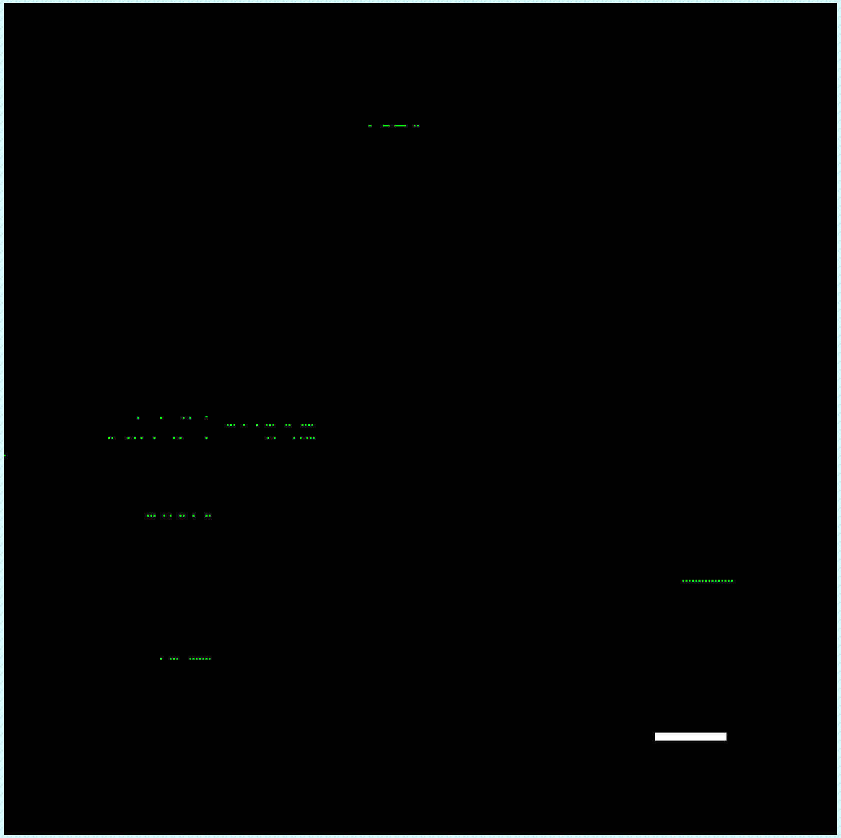

Multiple passages of Sirius (α Canis Majoris) captured by a QCE camera connected to N150/750 telescope with 2X Barlow lens (scale bar: 500 mas).

Insensitivity of QCE image sensor to seeing conditions (4) – deep space observations

Pillars of Creation images of: a) NASA’s Hubble Space Telescope (visible domain) and
b) NASA’s James Webb Space Telescope (near-infrared domain).

Conclusions

- A modified Thomas Young's double-slit experiment was realized with Quantum Confinement Effect (QCE) image sensor. Two types of diffracted photons have been discovered: (i)Type I with particle behavior and (ii) Type II with wave behavior.

- The angular resolution of telescope due to Type I diffracted photons was investigated. Indoor measurements of the angular resolution have reached 16.5 milliarcseconds, an improvement of 50 x towards diffraction limit for a N150/750 telescope with 2X Barlow lens.

- Imaging through the atmosphere is improved by QCE image sensor due Type I diffracted photons with particle behavior. Sirius (α Canis Majoris) passage measurements have indicated seeing conditions estimated at 11 milliarcseconds. A novel concept is proposed to eliminate the seeing effects of atmospheric turbulence and to impulse the deep space investigations (nebulae, exoplanets, galaxy clusters, etc.).

Thank you for your attention!